

Original Article

Bilateral peripheral neural activity observed in vivo following unilateral nerve injury

Deepak Behera*, Subrat Behera*, Kathleen E Jacobs, Sandip Biswal

Department of Radiology, Molecular Imaging Program at Stanford, 300 Pasteur Drive S-062B, Stanford University, CA 94304, California, USA. *These authors contributed equally to this work.

Received February 25, 2013; Accepted March 12, 2013; Epub April 9, 2013; Published April 15, 2013

Abstract: Manganese-enhanced magnetic resonance imaging (MRI) is a surrogate method to measure calcium content in nervous system since manganese physiologically follows calcium. Manganese is detectable in MRI and therefore visualizes structures and cell populations that actively regulate calcium. Since calcium is actively recruited for the transmission of action potentials, our purpose is to validate manganese-enhanced MRI for detection of changes in lumbar nerves related to nociception. A neuropathic pain model was created by chronic constrictive injury of the left sciatic nerve of Sprague-Dawley rats. Behavioral measurements, using von Frey's tests, confirmed the presence of significant allodynia in the left hind limb of animals in the injured group. T1-weighted fast spin echo images were obtained of the lumbar cord and plexus of animals with injured left sciatic nerve and uninjured animals (control) scanned in a 7 Tesla magnet after intraperitoneal manganese chloride administration four weeks after surgery. Lumbar nerve roots and sciatic nerves in the injured group show increased normalized manganese-enhanced MRI signal, representing manganese enhancement, compared to the control group. In conclusion, animals with neuropathic pain in the left hind limb show increased manganese uptake in not only the injured sciatic nerve but also in the contralateral uninjured sciatic nerve on manganese-enhanced MRI in vivo. Although poorly understood, this finding corroborates ex vivo finding of bilateral nociceptive-related molecular changes in the nervous system of unilateral pain models.

Keywords: Manganese-enhanced magnetic resonance imaging, chronic constrictive injury, sciatic nerve injury, neuropathic pain, animal model

Introduction

In the past several years, manganese-enhanced magnetic resonance imaging (MEMRI) has emerged as a powerful surrogate marker for imaging calcium flux into tissues. Manganese (Mn), a T1 shortening agent and a surrogate magnetic resonance (MR) marker for calcium, can be used as a MR contrast agent as it enters active neuronal cells through voltage-gated calcium channels [1]. MEMRI can accurately depict stimulus-induced regional activation in certain tissues. Previous work by others has shown that the rate of manganese accumulation is higher in active neuronal populations compared to quiescent cells [2-5]. This phenomenon has been referred to as either activation-induced manganese-enhanced MRI (AIM MRI) or dynamic activity-induced manga-

nese-dependent contrast MRI (DAIM MRI) [6, 7]. Using these techniques, investigators have been able to localize manganese enhancement of specific neuronal or cardiac structures that have been purposefully stimulated [6].

Since actively firing pain-sensing neurons rely upon calcium fluxes for propagation of the pain signal, we hypothesize MEMRI has the potential to image heightened nociceptive activity in the central and peripheral nervous system. The ability to functionally image such neuronal behavior would be helpful in objectively and functionally identifying neural structures associated with pain generation.

Our objective was to validate MEMRI for detection of peripheral nerve nociceptive activity in a rat model of neuropathic pain. A well estab-

Bilateral peripheral neural activity following unilateral nerve injury

lished rat neuropathic pain model is one where the sciatic nerve is injured by chronic compression using surgical sutures [8], known as the Chronic Constrictive Injury (CCI) model. We evaluated MEMRI signal intensity in the sciatic nerves in the CCI model and compared it to that in uninjured control subjects. While the results of this study do not specifically identify the nociceptive pathway responsible, the approach used does localize the tracts involved and perhaps objectively identifies the neuroanatomic level of injury.

Material and methods

Neuropathic pain model

Animal experiments were approved by Stanford IACUC. Experiments were carried out using adult male Sprague-Dawley rats weighing 200-250 g. There were two experimental groups: 1) A CCI group, which consists of animals undergoing a left Chronic Constrictive Injury (CCI) of the sciatic nerve procedure (n=5), 2) A control group of asymptomatic non-operated animals (n=3). We utilized the Chronic Constrictive Injury (CCI) model, a well-characterized rat neuropathic pain model described by Bennett and Xie [8].

Briefly, animals were anesthetized with inhalational 2-3% isoflurane and placed on a warming bed. Hair was removed from the posterolateral aspect of the left thigh. Following a longitudinal skin incision at mid thigh level, the left sciatic nerve was identified, exposed and four loose ligatures were placed on it. This procedure provokes a chronic mechanical and thermal hypersensitivity; symptoms usually persist from 1 week to 8 weeks after surgery, then reduce in intensity over the next 4 weeks [8]. After surgery, procedures and injections, all animals were returned to their cages and allowed free access to food and water. Animals were permitted to heal for four weeks after the surgery in isolation from other animals.

Manganese-enhanced MRI

MR images of all animals were obtained before (baseline) and twenty-four hours after intraperitoneal (IP) injection of manganese chloride ($MnCl_2$; 30 mM solution; 1 ml per 100 gm of body weight). Manganese-enhanced MRI, (MEMRI) was performed 24 hours after manga-

nese chloride injection to allow sufficient time for absorption from intraperitoneal space. Also, studies on brain MEMRI suggest a 24-hour period is required for attaining equilibrium of manganese distribution in the brain [1]. After injection with $MnCl_2$, animals were returned to their cages and allowed free access to food and water.

All MRI experiments were performed on a self-shielded 30-cm-bore 7-T small animal MR imaging unit (Varian) with a 9-cm-bore gradient insert (Resonance Research Inc.) using EXCITE2 electronics and the supporting LX11 platform (GE Healthcare). Animals were placed in a rodent holder and then into a 7 cm bore quadrature volume transmit/receive RF coil, which was centered on the lumbosacral region. The animals were anesthetized with humidified, oxygen-enriched 2-3% isoflurane (inhalation (IH)) administered via nose cone. Temperature and respiration were carefully monitored during imaging. The animals were kept warm during the imaging procedure by maintaining the ambient air temperature within the scanner bore at 34°C. T1-weighted fast spin echo images (TR/TE 800/7.7 ms echo train length 8, 31.1 kHz bandwidth, NEX 4, FOV 6 cm, 256x256 pixels, in-plane resolution 234 μm^2 , slice thickness 1 mm) were obtained.

Regions of interest (ROIs) (RT_Image image analysis software, version 0.6.1b, source: Edward Graves, Department of Radiation Oncology, Stanford University School of Medicine) were placed on sciatic nerves bilaterally, just inferior to L6 vertebra, at the level of sacral promontory to quantify the degree of manganese enhancement, and were normalized to background signal in the muscle (normalized signal) (**Figure 1**). From the T1-weighted spin echo images, 3D maximum intensity projections of the lumbar cord plexus were generated (Osirix image analysis software, version 3.7.1, source: <http://www.osirix-viewer.com>).

Pain behavior assessment

Development of allodynia in the CCI model was evaluated during the third week after surgery by assessing mechanical allodynia using Semmes Weinstein von-Frey Hair filaments (Stoelting Co., Wood Dale, IL, USA). Sensitivity to mechanical stimulation was measured by

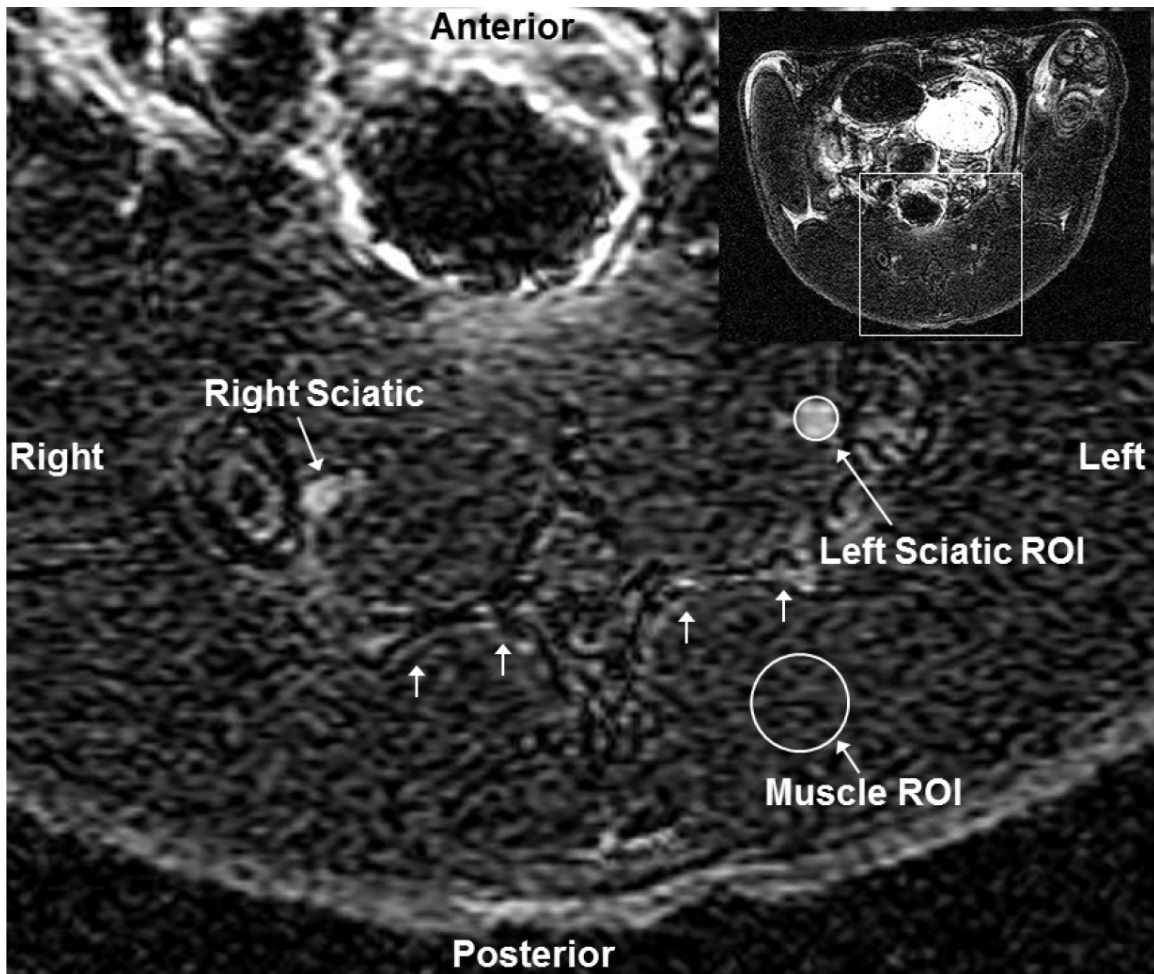


Figure 1. Placement of ROIs around sciatic nerves. Axial T1 weighted MRI slice of the posterior rat pelvis (inset image of entire transaxial slice shown in upper right corner) showing sacrum (multiple small arrows), right and left sciatic nerves, representative regions-of-interest (ROI) around the left sciatic nerve and muscle. Inset shows the entire slice from which the magnified slice was obtained.

recording the paw withdrawal response to serially increasing filament stiffness.

The animals were placed on a raised platform with a mesh floor for the test. They were acclimated to the platform for two hours each for four days prior to testing and an hour just before testing. The filament was applied to the lateral portion of plantar aspect of both hind paws through the mesh floor until it bent and kept in place for eight seconds. A positive response was recorded if the animal withdrew the paw briskly off the floor in response to the application. An application with the same filament was repeated at a minimum interval of 60 seconds if it produced a positive response. Testing of the paw was terminated if it showed 3 consecutive positive responses for a single filament or if

the filament lifted the paw off the floor, in which case it was scored as 3 positive responses.

The data thus collected was analyzed using the Psychofit program (source: <http://psych.colorado.edu/~lharvey/html/software.html>), which computes a maximum-likelihood fit of a sigmoid psychometric function to empirical data and calculates the withdrawal threshold in log filament stiffness units. The threshold is defined as the stimulus intensity at which the withdrawal is detected 50% of the time [9-11].

Statistical analysis

Differences in paw-withdrawal thresholds between left and right paws were tested separately for CCI and control groups using two-

Bilateral peripheral neural activity following unilateral nerve injury

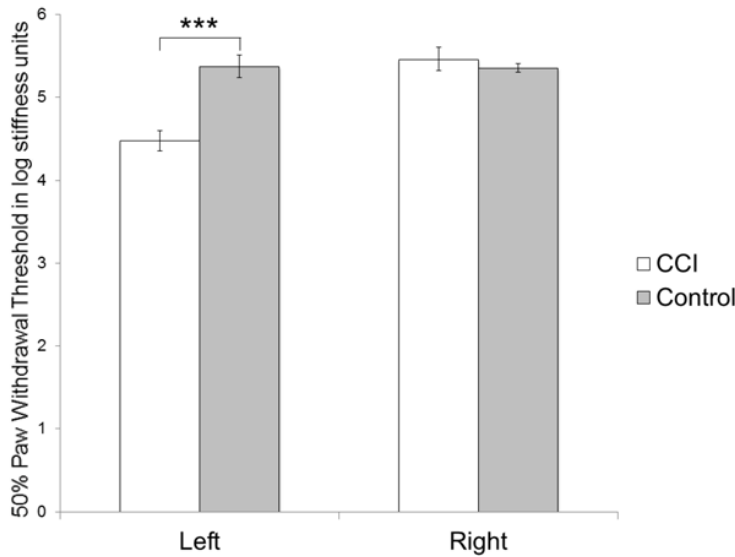


Figure 2. Measurements of allodynia. Von Frey's test shows increased sensitivity to mechanical stimulation in the operated paw (left) in the CCI group as evidenced by a reduction in the paw withdrawal threshold compared to the non-operated paw (right) or either paws in the control group (***p*<0.002).

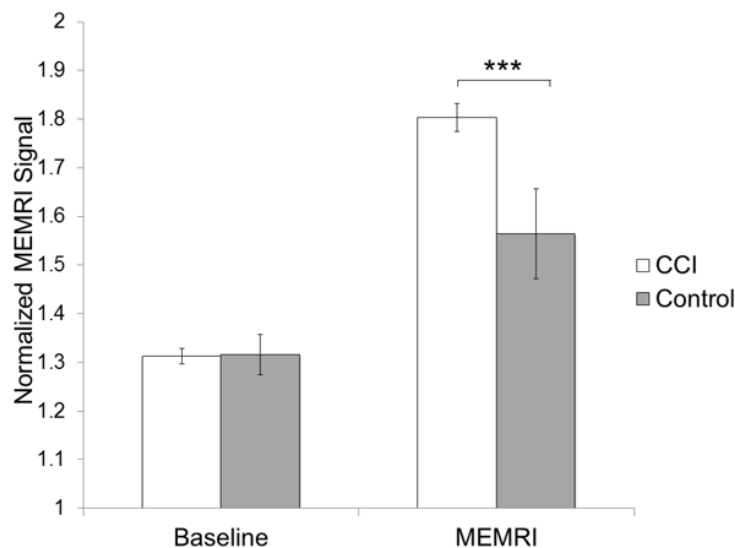


Figure 3. Normalized MEMRI signal in sciatic nerves. Average normalized MEMRI signal (\pm s.e.m) in peripheral nerves is increased in response to Chronic Constrictive Injury (CCI) (***p*<0.01).

tailed paired t-tests. Differences in normalized MRI signal between CCI and control groups were tested separately for each side with a one-sided Mann-Whitney U test. The level of statistical significance was set at *p*<0.05. Statistical analyses were done using online statistical tools (<http://faculty.vassar.edu/lowry/VassarStats.html>) and excel spreadsheets.

Results

Confirmation of pain behavior

Clinical evidence of development of allodynia in the CCI group was demonstrated by lower paw withdrawal thresholds, illustrated using the von-Frey Hair test. Behavioral measurements showed significantly lower paw withdrawal thresholds in the left hindpaws (4.48 ± 0.26 log stiffness units) of the CCI group compared to the right hindpaws (5.46 ± 0.32) (*p*<0.002). Paw withdrawal thresholds were not different between both paws in control animals (in log stiffness units - left hindpaws: 5.32 ± 0.19 ; right hindpaws: 5.31 ± 0.1 ; *p*>0.9), but were similar to those in uninjured right hindpaws in the CCI group (**Figure 2**).

Sciatic nerves of the CCI animals show increased MEMRI signal intensity

MEMRI showed increased signal in the distal spinal cord and peripheral nervous systems in animals with CCI. **Table 1** shows means, standard deviations and sample sizes of normalized peripheral (sciatic) nerve signal. Prior to manganese administration, baseline MRI showed similar normalized sciatic nerve signals in the CCI and control groups (normalized signal - CCI: left hindpaw 1.35 ± 0.04 , right hindpaw 1.28 ± 0.04 ; Control: left hindpaw 1.31 ± 0.09 , right hindpaw 1.32 ± 0.13). Following manganese administration, MEMRI showed significant difference between the normalized nerve signals in the CCI and control groups.

The CCI group showed a higher signal than the control group in the sciatic nerves on the operated left side (CCI: 1.83 ± 0.09 , Control: 1.55 ± 0.27 ; *p*<0.01) as well as the unoperated right side (CCI: 1.78 ± 0.09 , Control: 1.58 ± 0.24 ; *p*<0.03) (**Figure 3**). Representative axial images through the posterior pelvis are shown in **Figure 4**.

Bilateral peripheral neural activity following unilateral nerve injury

Table 1. Means, Standard Deviations and Sample Sizes of normalized peripheral nerve MEMRI Signal on each side

	Group	Statistic	Operated/Left Nerve	Unoperated/Right Nerve	Combined
Baseline	CCI	Mean	1.35	1.28	1.31
		SD	0.04	0.04	0.05
		N	5	5	10
	Control	Mean	1.31	1.32	1.32
		SD	0.09	0.13	0.10
		N	3	3	6
	Combined	Mean	1.33	1.30	1.31
		SD	0.06	0.08	0.07
		N	8	8	16
MEMRI	CCI	Mean	1.83	1.78	1.80
		SD	0.09	0.09	0.09
		N	5	5	10
	Control	Mean	1.55	1.58	1.56
		SD	0.27	0.24	0.23
		N	3	3	6
	Combined	Mean	1.72	1.70	1.71
		SD	0.22	0.18	0.19
		N	8	8	16

MEMRI=Manganese Enhance MRI. CCI=Chronic Constrictive Injury.

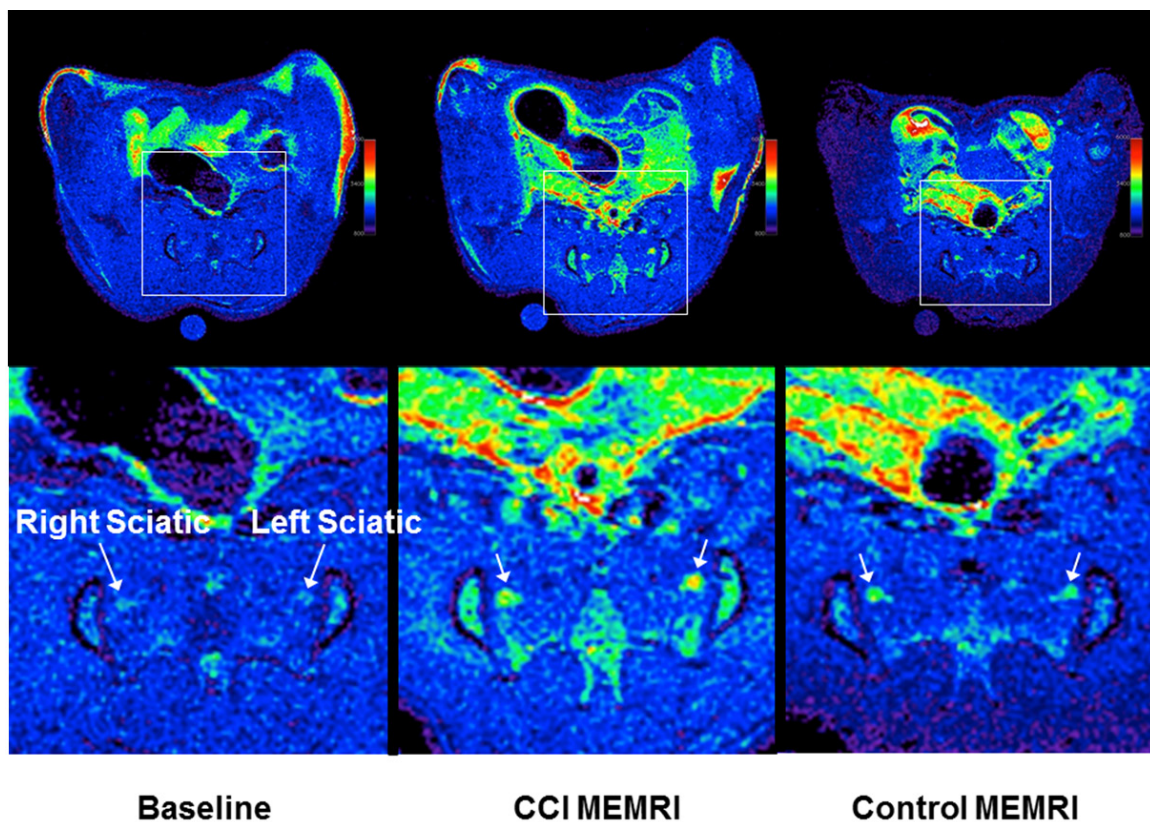


Figure 4. Transaxial images of a representative baseline scan, and representative MEMRI scans from each group showing the sciatic nerves in the pelvis anterior to the sacrum. The top row shows the entire slice while the bottom row zooms into the relevant part as marked by boxes in the top row. All images are similarly windowed. MEMRI improves the signal in both groups over baseline. In MEMRI, the CCI animal shows higher signal intensity in the sciatic nerve than the control animal. The higher signal relative to the surrounding muscle makes the nerves more visible in the CCI MEMRI.

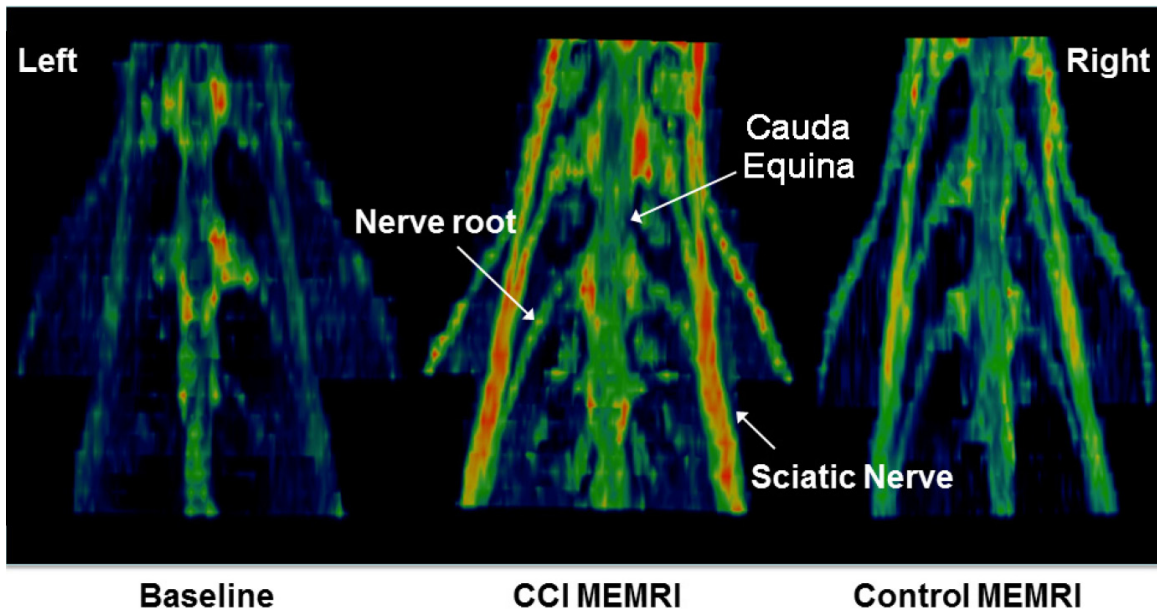


Figure 5. Reconstructed MEMRI views of the lumbar plexus. Normalized 3D maximum intensity projection (MIP) images (posterior projection) of a representative baseline scan, and representative MEMRI scans from each group showing the lumbar spinal cord, cauda equina and lumbar plexus. MEMRI improves the signal in both groups over baseline. In MEMRI, the CCI animal shows higher signal intensity in the peripheral nerves of the lumbar plexus than the control animal.

3D maximum intensity projections of the lumbar cord plexus were produced from the fast spin echo images and show increased enhancement of the lumbar cord and plexus in the animals following manganese administration, when compared to baseline. Further, greater manganese enhancement of the lumbar cord and plexus is seen in the CCI group compared to the control group (Figure 5).

Increased MEMRI signal in the sciatic nerve of CCI animals has good correlation with increased allodynia. The 50% paw withdrawal threshold has a moderately good negative linear correlation with normalized MEMRI signal in the sciatic nerve ($r^2=0.659$).

Discussion

Chronic pain states result in activation and/or elevation in the number of certain calcium channels in nociceptive neurons [12], for instance, the high-voltage gated N-channel [13, 14], the low-voltage gated T-channel [15, 16], the non-selective cation channel transient receptor potential cation channel subfamily V member 1 (TRPV1) [17, 18], etc. Although not specific to any one type of calcium channel,

results from our study indicate that MEMRI can be used to functionally highlight and objectively identify active peripheral neuronal pathways in a rat model of neuropathic pain. MEMRI utilizes physiological changes, specifically 'sensitization' occurring in chronic pain to functionally highlight both the pain-sensing neurons and its contralateral non-injured neural counterpart.

We are able to demonstrate higher MEMRI signal in peripheral nerves in animals experiencing pain. However, we also observed an increase in T1-weighted signal enhancement on the non-injured side, contralateral to the nerve injury in the CCI group. Events that effect nonlesioned structures contralateral to a peripheral nerve lesion is a well documented phenomenon described in rats [19]. Although the exact mechanism is not yet known, it has been shown that unilateral axotomy results in bilateral changes in levels of mRNA for cholecystokinin [20], and bilateral changes in the neuropeptides galanin, neuropeptide Y and vasoactive intestinal polypeptide [21]. These changes might be related to bilateral increases in trophic factors like nerve growth factor (NGF) that have been measured following unilateral axotomy [22]. There are numerous studies that have

Bilateral peripheral neural activity following unilateral nerve injury

found similar bilateral neuroinflammatory reaction in response to unilateral nerve injury while showing only ipsilateral mechanical allodynia [23-25]. Further, studies indicate that after nerve injury, contralateral allodynia increases in a time-dependent manner, with a delayed onset, in the un-injured side [26, 27]. These studies suggest that behavioral manifestation of pain on the side contralateral to the nerve injury may follow more basic neuroinflammatory changes at the molecular and receptor level. Regardless of the exact mechanism, the increase in enhancement seen contralaterally to the source of pain in the CCI group on the 3D maximal intensity projections in our study is likely partly attributable to this phenomenon.

Additionally, the observation of enhancement contralateral to the site of injury might be considered a limitation of this method, but the fact that the image was obtained 24 hours after $MnCl_2$ administration may indeed reflect manganese equilibrium attained in both the injured and contralateral nerves. If we were to obtain images relatively sooner (<24 hours), it may be possible to see preferential manganese accumulation in the ipsilateral injured nerve when compared to the contralateral nerve due to differential rates of manganese uptake. Ongoing experiments are currently addressing these issues and studying neural activity in both intact and injured peripheral nerves. We are also studying the effect of analgesic treatments on MEMRI signal.

Recognizing active nociceptive peripheral nerves using MEMRI may help inform diagnostic and therapeutic decisions. The diagnosis of peripheral nerve entrapment syndromes, such as carpal tunnel syndrome and piriformis syndrome, can potentially be aided by MEMRI when diagnosis can be challenging in early stages of the disease. Additionally, MEMRI may provide more objective decision support for fluoroscopy, computed tomography, or ultrasound-guided local anesthetic and steroid injections that are currently used to empirically treat a large variety of clinical pain disorders including low back pain, sciatica, post-surgical pain, post-traumatic neuralgia, etc.

In addition to helping guide therapeutic decisions, MEMRI can also be used to screen drug candidates for analgesia. Novel therapeutic strategies targeted on the peripheral mecha-

nisms of neuropathic pain (for example, blocking ion channels in peripheral neurons, modulation of peripheral excitability via cannabinoid receptors, blocking glutamate receptors in spinal cord, blocking activated spinal neuroglia, etc) [28] may find MEMRI to be a useful tool for evaluation of efficacy and local targeting.

Of note, manganese, which is essential for cell viability at normal levels, is toxic in humans at high concentrations [29-33]. Chronic manganese exposure causes 'manganism' [34], a movement disorder similar to Parkinson's disease, which has limited its translation into the clinic. However, recent developments look promising for use in patients. For example, mangafodipir trisodium (MnDPDP; Teslascan) is an FDA-approved MRI contrast agent consisting of chelated manganese for MRI evaluation of the liver, which showed no significant adverse effects in its clinical trials [35].

As technology advances and newer developments allow for manganese to provide contrast at lower concentrations, manganese-based imaging may emerge as the means of diagnosing and assessing the severity of neuropathic and other forms of chronic pain in human subjects in the future. MEMRI could potentially benefit living subjects with neuropathic and, perhaps, other chronic pain syndromes by offering scientists and health care providers a noninvasive tool to study pre-clinical and clinical pain syndromes, determine the effectiveness of systemic analgesics, and provide vital information useful in treating pain with image-guided regional nerve blockade or other novel minimally invasive approaches.

Conclusions

Animals with neuropathic pain in the left hind limb show increased manganese uptake in the lumbar plexus on MEMRI in vivo, which correlates with the development of allodynia. This approach can be used as a tool to study nociceptive activity and related physiological changes in neuropathic pain models.

Abbreviations

CCI, Chronic Constrictive Injury; IH, inhalation; IP, intraperitoneal; MEMRI, manganese-enhanced MRI; MIP, maximum intensity projection; MRI, magnetic resonance imaging; ROI, region of interest.

Acknowledgements

Authors' contributions: DB, SB and KJ helped in the surgeries, imaging and behavioral tests of the animals, compiled, analyzed and interpreted the data, and drafted the manuscript. DB and SB participated in the study design and coordination, and they helped to draft the manuscript.

We would like to thank Drs. Dirk B. Mendel and Steve Harrison, both previously of Kai Pharmaceuticals, for their support and guidance. We would also like to acknowledge and thank Drs. Laura Pisani and Tim Doyle for their assistance with the small animal MRI in the Small Animal Imaging Core at Stanford University.

Competing interests

The authors have no competing interests for the work described here.

Address correspondence to: Sandip Biswal, Department of Radiology, Molecular Imaging Program at Stanford, 300 Pasteur Drive S-068B, Stanford, CA 94305, USA. Phone: 650-498-4561; Fax: 650-725-7296; E-mail: biswals@stanford.edu

References

- [1] Silva AC, Lee JH, Aoki I and Koretsky AP. Manganese-enhanced magnetic resonance imaging (MEMRI): methodological and practical considerations. *NMR Biomed* 2004; 17: 532-543.
- [2] Aschner M and Aschner JL. Manganese neurotoxicity: cellular effects and blood-brain barrier transport. *Neurosci Biobehav Rev* 1991; 15: 333-340.
- [3] Drapeau P and Nachshen DA. Manganese fluxes and manganese-dependent neurotransmitter release in presynaptic nerve endings isolated from rat brain. *J Physiol* 1984; 348: 493-510.
- [4] Kita H, Narita K and Van der Kloot W. Tetanic stimulation increases the frequency of miniature end-plate potentials at the frog neuromuscular junction in Mn²⁺-, CO₂⁺-, and Ni²⁺-saline solutions. *Brain Res* 1981; 205: 111-121.
- [5] Narita K, Kawasaki F and Kita H. Mn and Mg influxes through Ca channels of motor nerve terminals are prevented by verapamil in frogs. *Brain Res* 1990; 510: 289-295.
- [6] Aoki I, Tanaka C, Takegami T, Ebisu T, Umeda M, Fukunaga M, Fukuda K, Silva AC, Koretsky AP and Naruse S. Dynamic activity-induced manganese-dependent contrast magnetic resonance imaging (DAIM MRI). *Magn Reson Med* 2002; 48: 927-933.
- [7] Lin YJ and Koretsky AP. Manganese ion enhances T1-weighted MRI during brain activation: an approach to direct imaging of brain function. *Magn Reson Med* 1997; 38: 378-388.
- [8] Bennett GJ and Xie YK. A peripheral mononeuropathy in rat that produces disorders of pain sensation like those seen in man. *Pain* 1988; 33: 87-107.
- [9] Berquin AD, Lijesevic V, Blond S and Plaghki L. An adaptive procedure for routine measurement of light-touch sensitivity threshold. *Muscle Nerve* 2010; 42: 328-338.
- [10] Gescheider GA. *Psychophysics Method, Theory, and Application*. Hillsdale, NJ: Lawrence Erlbaum Associates 1985.
- [11] Plaghki L and Mouraux A. Fonctions psychométriques et méthodes psychophysiques adaptatives pour l'étude de la douleur. *Douleur et Analgesie* 2001; 14: 73-77.
- [12] Yaksh TL. Calcium channels as therapeutic targets in neuropathic pain. *J Pain* 2006; 7: S13-30.
- [13] Saegusa H, Kurihara T, Zong S, Kazuno A, Matsuda Y, Nonaka T, Han W, Toriyama H and Tanabe T. Suppression of inflammatory and neuropathic pain symptoms in mice lacking the N-type Ca²⁺ channel. *Embo J* 2001; 20: 2349-2356.
- [14] Snutch TP. Targeting chronic and neuropathic pain: the N-type calcium channel comes of age. *NeuroRx* 2005; 2: 662-670.
- [15] Ikeda H, Heinke B, Ruscheweyh R and Sandkuhler J. Synaptic plasticity in spinal lamina I projection neurons that mediate hyperalgesia. *Science* 2003; 299: 1237-1240.
- [16] Matthews EA and Dickenson AH. Effects of ethosuximide, a T-type Ca(2+) channel blocker, on dorsal horn neuronal responses in rats. *Eur J Pharmacol* 2001; 415: 141-149.
- [17] Ramsey IS, Delling M and Clapham DE. An introduction to TRP channels. *Annu Rev Physiol* 2006; 68: 619-647.
- [18] Vellani V, Mapplebeck S, Moriondo A, Davis JB and McNaughton PA. Protein kinase C activation potentiates gating of the vanilloid receptor VR1 by capsaicin, protons, heat and anandamide. *J Physiol* 2001; 534: 813-825.
- [19] Koltzenburg M, Wall PD and McMahon SB. Does the right side know what the left is doing? *Trends Neurosci* 1999; 22: 122-127.
- [20] Verge VM, Wiesenfeld-Hallin Z and Hokfelt T. Cholecystokinin in mammalian primary sensory neurons and spinal cord: in situ hybridiza-

Bilateral peripheral neural activity following unilateral nerve injury

- tion studies in rat and monkey. *Eur J Neurosci* 1993; 5: 240-250.
- [21] Zhang X, Ji RR, Arvidsson J, Lundberg JM, Bartfai T, Bedecs K and Hokfelt T. Expression of peptides, nitric oxide synthase and NPY receptor in trigeminal and nodose ganglia after nerve lesions. *Exp Brain Res* 1996; 111: 393-404.
- [22] Ramer M and Bisby M. Reduced sympathetic sprouting occurs in dorsal root ganglia after axotomy in mice lacking low-affinity neurotrophin receptor. *Neurosci Lett* 1997; 228: 9-12.
- [23] Dubovy P, Klusakova I, Svizenska I and Brazda V. Spatio-temporal changes of SDF1 and its CXCR4 receptor in the dorsal root ganglia following unilateral sciatic nerve injury as a model of neuropathic pain. *Histochem Cell Biol* 2010; 133: 323-337.
- [24] Jancalek R, Dubovy P, Svizenska I and Klusakova I. Bilateral changes of TNF-alpha and IL-10 protein in the lumbar and cervical dorsal root ganglia following a unilateral chronic constriction injury of the sciatic nerve. *J Neuroinflammation* 2010; 7: 11.
- [25] Brazda V, Klusakova I, Svizenska I, Veselkova Z and Dubovy P. Bilateral changes in IL-6 protein, but not in its receptor gp130, in rat dorsal root ganglia following sciatic nerve ligation. *Cell Mol Neurobiol* 2009; 29: 1053-1062.
- [26] Takaishi K, Eisele JH Jr, Carstens E. Behavioral and electrophysiological assessment of hyperalgesia and changes in dorsal horn responses following partial sciatic nerve ligation in rats. *Pain* 1996; 66: 297-306.
- [27] Tabo E, Jinks SL, Eisele JH Jr and Carstens E. Behavioral manifestations of neuropathic pain and mechanical allodynia, and changes in spinal dorsal horn neurons, following L4-L6 dorsal root constriction in rats. *Pain* 1999; 80: 503-520.
- [28] Dray A. Neuropathic pain: emerging treatments. *Br J Anaesth* 2008; 101: 48-58.
- [29] Wolf GL, Baum L. Cardiovascular toxicity and tissue proton T1 response to manganese injection in the dog and rabbit. *AJR Am J Roentgenol* 1983 Jul; 141: 193-7.
- [30] Barbeau A, Inoue N and Cloutier T. Role of manganese in dystonia. *Adv Neurol* 1976; 14: 339-352.
- [31] Chandra SV, Shukla GS and Saxena DK. Manganese-induced behavioral dysfunction and its neurochemical mechanism in growing mice. *J Neurochem* 1979; 33: 1217-1221.
- [32] Gorell JM, Johnson CC, Rybicki BA, Peterson EL, Kortsha GX, Brown GG and Richardson RJ. Occupational exposures to metals as risk factors for Parkinson's disease. *Neurology* 1997; 48: 650-658.
- [33] Wang JD, Huang CC, Hwang YH, Chiang JR, Lin JM and Chen JS. Manganese induced parkinsonism: an outbreak due to an unrepaired ventilation control system in a ferromanganese smelter. *Br J Ind Med* 1989; 46: 856-859.
- [34] Zhao F, Cai T, Liu M, Zheng G, Luo W and Chen J. Manganese induces dopaminergic neurodegeneration via microglial activation in a rat model of manganese toxicity. *Toxicol Sci* 2009; 107: 156-164.
- [35] Federle MP, Chezmar JL, Rubin DL, Weinreb JC, Freeny PC, Semelka RC, Brown JJ, Borello JA, Lee JK, Mattrey R, Dachman AH, Saini S, Harmon B, Fenstermacher M, Pelsang RE, Harms SE, Mitchell DG, Halford HH, Anderson MW, Johnson CD, Francis IR, Bova JG, Kenney PJ, Klippenstein DL, Foster GS and Turner DA. Safety and efficacy of mangafodipir trisodium (MnDPDP) injection for hepatic MRI in adults: results of the U.S. multicenter phase III clinical trials (safety). *J Magn Reson Imaging* 2000; 12: 186-197.